



Filtration of subcritical water hydrolysates from red macroalgae byproducts with ultraporous ceramic membranes for oligosaccharide and peptide fractionation

E. Trigueros, M.T. Sanz, S. Beltrán, M.O. Ruiz^{*}

Department of Biotechnology and Food Science, Chemical Engineering Division, University of Burgos, Plza. Misael Bañuelos s/n, 09001, Burgos, Spain

ARTICLE INFO

Keywords:

Peptide purification
Oligosaccharide recovery
Membrane fouling
Macroalga byproducts
Biorefinery

ABSTRACT

An ultrafiltration-based process for oligosaccharide and peptide fractionation from a macroalgae subcritical water hydrolysate was studied. A wide range of separation results was obtained depending on the membrane pore. 100 kDa cut-off size was enough for hydrolysate clarification with total retention of colloidal materials. Oligosaccharides present in the hydrolysate showed the highest retention with all membranes, glucans mostly, followed by galactans, and finally arabinans. Peptides obtained after subcritical water treatment were some of the lowest rejected compounds, even using a 5 kDa membrane. The increase in temperature from 20 to 50 °C and feed flow rate from 6.6 to 11.2 L/h enhanced permeate flux for 5 kDa membrane, without perturbing the membrane retention. The Hermia's models identified the cake layer resistance as the major fouling resistance in hydrolysate filtrations at 20 °C, but standard pore blockage was the principal fouling mechanism at 50 °C. A fractionation process with sequential filtration stages at 20 °C and TMP = 1.1 bar was examined. Oligosaccharides were fractionated in the retentates of the sequential filtrations with 100, 5 and 1 kDa membranes. The final permeate collected from the 1 kDa membrane was freeze-dried to obtain a peptide-rich solid (71 wt%) that could be used in different applications.

1. Introduction

Red marine seaweeds are frequently exploited due to their high content of phycocolloids, such as agar and carrageenans. Agar is a hydrocolloid that forms a thermo-reversible gel when it is dissolved in hot water and cooled [1]. It is widely used in different areas such as microbiology, pharmacy, food, or cosmetics [2]. *Gelidium sesquipedale* is the major seaweed resource in the Spanish agar industry since it provides the best raw material to obtain the highest quality agar [3]. The industrial agar extraction process involves the generation of a solid residue, which is usually discarded, despite containing a significant content of valuable compounds [4,5].

One profitable way of obtaining the highest benefit from this residue is by turning it into a valuable source of food additives and chemical compounds. For this purpose, subcritical water extraction/hydrolysis has been shown to have a great capacity to extract bioactive compounds from different natural sources [6,7]. Subcritical water (SW) is pressurized water in its liquid state in the temperature range from 100 °C to 374 °C. Under these conditions, water presents unique properties such as

higher ionic product and lower dielectric constant than at ambient conditions [8]. The use of SW to valorize the solid residue of *Gelidium sesquipedale* after agar extraction has been previously reported by Trigueros *et al.* [9]. Nearly 100% of the protein fraction was extracted and hydrolysed by using a semicontinuous reactor at 185 °C and a residence time of 3 min. However, subcritical water hydrolysates (SWH) are complex mixtures, which means that a suitable separation technique is required to recover, isolate, and concentrate valuable compounds. The nutritional and pharmaceutical value of oligosaccharides and peptides recovered in the hydrolysates from red macroalga justifies the interest in their separation and purification [10–12].

In this sense, pressure-driven membrane separation processes have been proven to be an environmentally friendly and cost-effective alternative for the recovery of different valuable compounds from byproducts [13,14]. Ultrafiltration (UF) is widely used for the separation of different molecules in solution based on molecular size, and to a lesser extent on molecular shape, charge, and hydrophobicity. Compounds commonly retained by UF membranes include suspended solids, proteins, peptides, polyphenols, polysaccharides, and some

^{*} Corresponding author.

E-mail address: moruiz@ubu.es (M.O. Ruiz).

<https://doi.org/10.1016/j.memsci.2022.120822>

Received 23 May 2022; Received in revised form 5 July 2022; Accepted 10 July 2022

Available online 21 July 2022

0376-7388/© 2022 The Authors. Published by Elsevier B.V. This is an open access article under the CC BY-NC-ND license (<http://creativecommons.org/licenses/by-nc-nd/4.0/>).

monosaccharides [13–15]. Easy automation and scale up, low energy costs, mild operation conditions, no use of toxic solvents and low waste generation are recognised as the main advantages of UF-based processes [16].

Different aqueous algae extracts obtained by conventional extraction (maceration) have already been fractionated using organic membranes with different pore sizes from 30 kDa to 300 kDa [17–19]. Denis et al. [17] found that a 30 kDa polyethersulfone tubular membrane was suitable to retain 100% of R-phycoerythrin of an extract from macroalgae *Grateloupia turuturu*, whereas Zaouk et al. [19] used a 50 kDa polyethersulphone membrane for the filtration of an aqueous extract from the red microalga *Porphyridium cruentum*. Ultraporous inorganic membranes, especially ceramics, are emerging as an alternative to conventional organic membranes due to their potential advantages, such as high chemical stability in a wide pH and temperature range, high wear resistance, long lifetime, and resistance to harsh chemical cleaning [20,21]. All these properties make inorganic membranes good candidates to be used for the treatment of SWH from red macroalgae solid residue, especially when a membrane system coupled to a reactor is desired.

Nevertheless, problems associated with UF membrane fouling remain the main disadvantage for its industrial implementation [22]. Some of the chemical compounds present in the SWH from *Gelidium sesquipedale* solid byproduct, such as oligosaccharides and peptides may play an important role in reversible and irreversible fouling, even when using crossflow filtration [14,23,24]. This dissolved matter, with high gelling properties, can cause severe fouling by accumulating in the pores and spreading over the surface of the membrane, which could lead to changes in membrane permeability and in retention coefficients along the separation treatment. The extent of fouling depends strongly on the SWH composition and concentration but can be significantly reduced by optimizing temperature and crossflow velocity [23,25]. Moreover, low transmembrane pressures are usually used in the filtration of colloidal, high viscosity, and multi-component solutions. It has already been reported that concentration polarization and membrane fouling become more important and lead to a high permeate flux drop when increasing operating pressure, as a result of the formation of less porous and more compacted cake layers [25,26]. Therefore, fractionation of the SWH by UF can lead to a valuable fraction rich with bioactive peptides.

Drying of the protein hydrolysate fraction will allow a more stable shelf-life product. In this regard, freeze-dried algae-protein products can exhibit commercial interest due to the wide range of application of algae-proteins in cosmetics, pharmaceuticals as well as food additives [27]. Freeze-drying has been examined because of its successful use in the preparation of products that must conserve their functional properties. In addition, the freeze-dried products usually show a good cake appearance, long lifetimes, a short reconstitution time and the same characteristics of the original liquid formulation after reconstitution [28].

This research has been carried out under the hypothesis of advancing on the use of the environmentally friendly membrane technology as a suitable purification process for the treatment of complex mixtures such as macroalgae subcritical water hydrolysates, as well as to improve the applicability of inorganic membranes. The aim of this study was to analyse the feasibility of continuous crossflow ultrafiltration with multi-channel ceramic membranes for the fractionation of subcritical water hydrolysates from *Gelidium sesquipedale* solid residue. The effect of pore size, temperature and feed flowrate on the separation yield and fouling was examined. A fractionation process to separate and recover oligosaccharides and peptides based on sequential ultrafiltration stages was proposed, followed by a final freeze-drying process to obtain a valuable powdered product rich in peptides.

2. Experimental

2.1. Chemicals and materials

Gelidium sesquipedale solid residue after industrial agar extraction was kindly provided by Hispanagar (Burgos, Spain). Glucose (99.5%), galactose (99%), arabinose (99%), ninhydrin (99%) and gallic acid (98%) were supplied by Sigma-Aldrich (USA). Sulfuric acid (96%) and iron (III) chloride were purchased from Merck (Spain); Folin-Ciocalteu's reagent, acetic acid and hydrochloric acid (37%) from VWR Chemicals (Germany); 2,4,6-Tri s(2-pyridyl)-1,3,5-triazine from Tokyo Chemical Industry; iron (II) sulphate 7-hydrate and potassium nitrate from Panreac PRS (Spain); sodium acetate from Scharlab (Spain); orthophosphoric acid (76%) and sodium hydroxide (99%) from Cofarcas S.A (Spain), and sodium carbonate (99.5%) from Honeywell Fluka (USA). Potassium hydrogen phthalate, sodium hydrogen carbonate, and sodium carbonate were provided by Nacalai Tesque INC (Japan). All chemicals were used without further purification.

Multichannel filtanium ceramic membranes with an active layer of TiO₂ supported on titania with a molecular weight cut-off size (MWCO) from 1 kDa to 100 kDa were supplied by TAMI Industries (France). These membranes consist of a single tubular module (254 mm length and 10 mm outside diameter) with seven inner channels (2 mm hydraulic diameter) and an effective membrane area, as stated by the manufacturer, of 132 cm². Note that TAMI membranes have a positive charge below pH 4–4.5, and a negative charge at higher pH values, with a point of zero charge at pH = 4–4.5 [29].

2.2. Subcritical water hydrolysis

SW experiments at pilot-scale level were carried out at Hiperbaric's facilities (Burgos, Spain) by using a discontinuous system. The main structural elements of the prototype were a reactor of 25 L capacity, a steam boiler as the heating system, a pump to recirculate and homogenize the biomass inside the reactor, a heat exchanger to avoid cooling during the recirculation process and a solid/liquid separation system. The maximum specifications were 185 °C and 20 bar. Operation and control of the process was performed by self-built Hiperbaric software. Before SW treatment, the dried macroalgae solid residue was milled by a cutting mill Retsch SM100 to reach a particle size lower than 0.5 mm according to the specifications of the recirculation pump. The biomass was first loaded in the reactor and then the pressurized water was added, keeping the macroalgae material in suspension during the process through a recirculation pump. SW hydrolysis was carried out at 175 °C (2.5% (w/v) biomass concentration) and a working pressure of 20 bar for 2 h. After extraction was finished, a filtration tank allowed phases separation to obtain a liquid hydrolysate and the solid residue. The liquid hydrolysate was the feed used in this work for fractionation by UF process.

2.3. Filtration assays by using membranes with different pore sizes

The retention degree of different compounds of the subcritical water hydrolysate (SWH) and their hydraulic resistance to filtration were determined. For that purpose, the hydrolysate and deionised water (conductivity < 15 µS/cm) were ultrafiltered with 5, 10, 50 and 100 kDa membranes. Additional tests were carried out with a 5 kDa membrane to evaluate the influence of temperature and feed flow rate on the fouling and separation capacity.

Crossflow filtration experiments were performed using the experimental setup shown in Fig. 1. The hydrolysate was continuously pumped from a hermetically sealed stirred feed tank (Pobel) to the membrane module, using a Masterflex peristaltic pump (HV-7520-57 with a Masterflex L/S Easy-Load II Head HV-77201-62). The pipes were silicone tubing Materflex L/S 15 (4.8 mm internal diameter). Before starting the filtration process, the feed solution was recirculated through the system

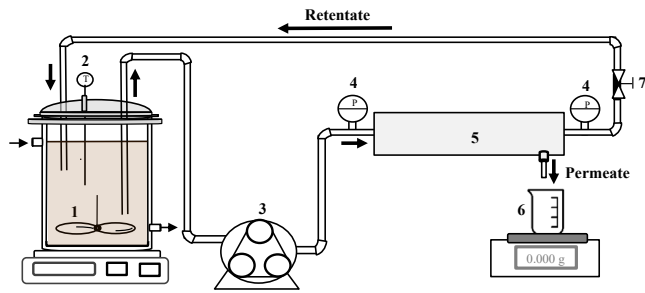


Fig. 1. Schematic diagram of the experimental setup for crossflow ultrafiltration experiments. 1. Feed jacked tank; 2. Thermometer; 3. Peristaltic pump; 4. Pressure gauge; 5. Tubular membrane module; 6. Permeate vessel; 7. Regulating recirculation valve.

for 15 min. Then, the feed flow rate and transmembrane pressure (TMP) were adjusted to the desired values by using the pump speed controller (from 6 to 600 rpm) and a valve placed after the membrane module. The pressures at the inlet and outlet of the membrane module were measured by using two pressure gauges.

All experiments were carried out by continuously withdrawing the permeate at constant TMP of 1.1 ± 0.2 bar. The retentate was recycled back to the feed tank and the permeate was collected in the permeate tank until the desired value of the volume reduction factor, VRF, was reached. The value of VRF was estimated during the ultrafiltration process as the ratio of the feed volume to the retentate volume ($VRF = V_F/V_R$). Permeate fluxes (J) were determined volumetrically (± 0.1 mL) and gravimetrically (± 0.001 g) at different operating conditions including MWCO, temperature and feed flow rate (Q_F). 11.2 L/h was used as the highest feed flow rate in order to avoid problems caused by foaming during SWH filtration.

All ceramic membranes were cleaned after each filtration experiment by the following cleaning procedure. First, the membrane was rinsed with deionised water (2 L) for 30 min, then cleaned with a 0.17 vol% aqueous H_3PO_4 solution for 60 min at 25 °C and 0.25 bar, and finally cleaned with a 0.20 g/L of NaOH solution for 90 min at 50 °C and 0.25 bar. The membrane was then rinsed with freshly deionised water and the permeate flux was measured at 20 °C under different pressures to check membrane cleaning. This cleaning procedure allowed to recover the initial water permeability coefficient of each membrane.

The filtration resistances have been estimated by the resistance-in-series model and Darcy's law (Eq. (1)) using the experimental values of J and TMP:

$$r_T = \frac{TMP}{J \cdot \mu} = r_m + r_f \quad (1)$$

where μ is the permeate viscosity (Pa·s), which depends on temperature, T (°C), in accordance with Eq. (2), r_T is the total resistance to filtration (m^{-1}), r_m is the membrane hydraulic resistance (m^{-1}) and r_f is the fouling resistance due to concentration polarization and fouling effects (m^{-1}). The resistance r_m was determined by performing ultrafiltration experiments with pure water at TMP from 0.25 to 2.5 bar and the contribution of the fouling to the total resistance, r_f/r_T , was calculated under different operating conditions.

$$\mu = \frac{0.479}{(T + 42.5)^{1.5}} \quad (2)$$

The Hermia's model [30] modified by Field et al. [31] for crossflow filtration, Eq. (3), has been employed to analyse the membrane fouling mechanisms:

$$\frac{dJ}{dt} = -k \cdot (J - J^*) \cdot J^{2-n} \quad (3)$$

where k is the fouling index, J^* can be considered as a critical flux that

should not be exceeded in order to avoid fouling, and n indicates the mechanism of fouling: $n = 2$ indicates the complete blocking model, $n = 1.5$ the standard blocking model, and $n = 0$ the cake layer model. When n is fixed, the following linearised fouling models were obtained by integrating Eq. (3) [31,32]:

$$\text{when } n = 2, \ln(J - J^*) = \ln(J_0 - J^*) - k_c \cdot t \quad (4)$$

$$\text{when } n = 1.5, \frac{1}{J^{0.5}} = \frac{1}{J_0^{0.5}} + k_s \cdot t \quad (5)$$

$$\text{when } n = 0, \ln\left(\frac{J}{J - J^*}\right) - \frac{J^*}{J} = \left[\frac{J^*}{J_0} - \ln\left(\frac{J_0 - J^*}{J_0}\right) \right] + k_{cl} \cdot J^{*2} \cdot t \quad (6)$$

where J_0 is the pure water flux ($m^3/(m^2 \cdot s)$), and k_c , k_s , k_{cl} are the fouling indexes for complete blocking (s^{-1}), standard pore-blocking ($m^{-0.5} s^{-0.5}$), and cake layer formation ($m^{-2} s$) models, respectively.

Eqs. (4)–(6) have been employed to fit the experimental permeate flux data. The most predominant fouling mechanism has been identified by comparing their determination coefficients, R^2 [31–33].

2.4. Experiments with sequential filtration stages

The flowchart of the integrated ultrafiltration process is shown in Fig. 2. Two independent cycles of sequential filtration stages were performed in order to determine the separation capacity and recovery factors. The feed solution was ultrafiltered through a 100 kDa membrane, obtaining a first permeate (p1) and retentate (r1). This first permeate p1 was then ultrafiltered through a 5 kDa membrane. Subsequently, the resulting permeate stream from 5 kDa membrane (p2) was subjected to lyophilisation to obtain the concentrated dry extract (Cycle A), while in Cycle B, p2 was ultrafiltered again through a 1 kDa membrane. The resulting permeate from the 1 kDa membrane (p3) was also lyophilized to obtain the concentrated dry extract for Cycle B. Samples of each permeate and retentate fraction were taken and stored at -18 °C for further analysis.

These filtrations were carried out at constant TMP of 1.1 ± 0.1 bar, Q_F of 11.2 L/h and 20 °C by continuously withdrawing the permeate. The retentate was recycled back to the feed tank during ultrafiltration. All ceramic membranes were cleaned before each experiment, following the aforementioned procedure, and the initial pure water flux was recovered in all cases.

2.5. Lyophilisation procedure

The final permeate fractions collected in the proposed sequential UF cycles were submitted to freeze-drying: p2 and p3 for Cycle A and B, respectively. First, samples were frozen with liquid nitrogen, equilibrated at -80 °C for 2 h and then submitted to freeze-drying in a Labconco Freeze Dry System (Labconco Corporation, U.S.A.) at $1.5 \cdot 10^{-7}$ bar during 48 h. The moisture content of the freeze-dried particles was determined gravimetrically by weighing small amounts of dried particles (around 0.5 g) before and after drying them in an oven at 105 °C until constant weight. The freeze-drying process yield was calculated as the ratio between the dried solid mass after the freeze-drying process and the total solid content of the final permeate of the multi-stage UF process. Each dried solid (S_A and S_B in Fig. 2) was then re-dissolved in deionised water to determine the final solid composition.

2.6. Analytical methods

Chemical and physical characterization was carried out for the SWH and the different fractions collected by UF, permeates and retentates.

The oligosaccharide fraction (OS) was quantified by high-performance liquid chromatography (HPLC) with a Biorad Aminex-HPX-87 H column (300×7.8 mm, Bio-Rad at 40 °C, a variable

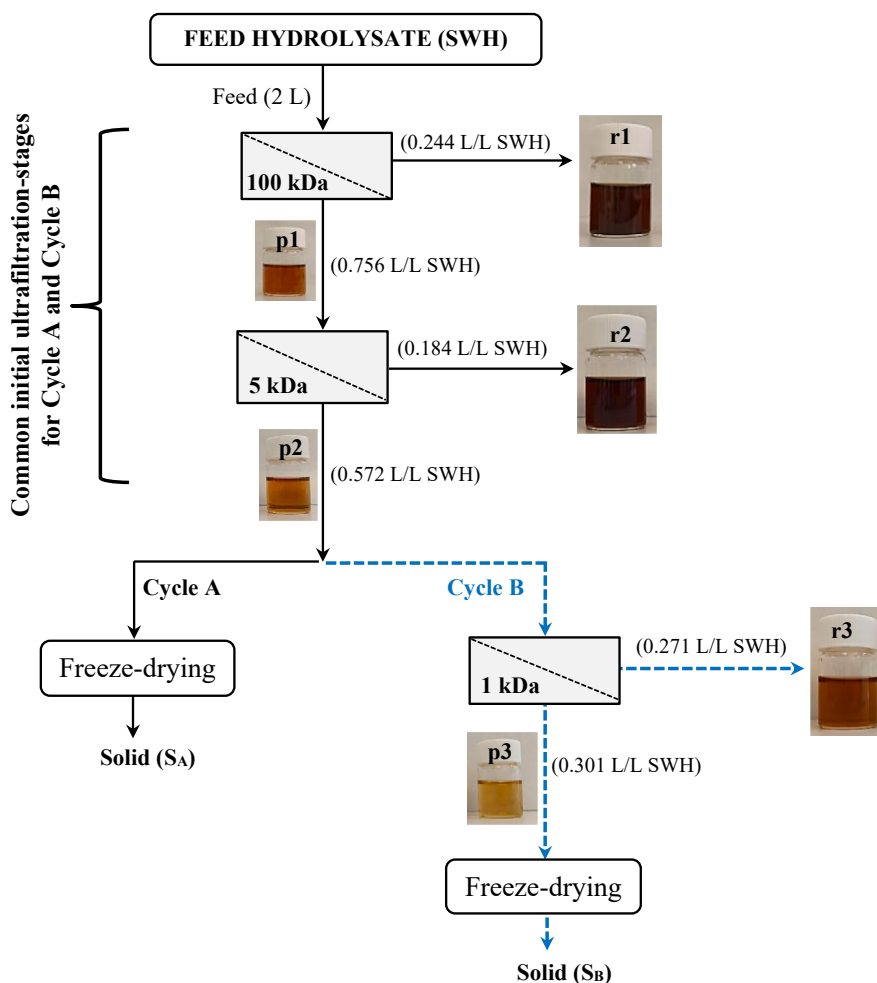


Fig. 2. Flowchart representing the sequential ultrafiltration performed for the separation of the oligosaccharide and peptide fractions from the subcritical water hydrolysate (SWH). The unit L/L refers to litre permeate or retentate obtained per litre of the SWH used as feed.

wavelength detector (VWD) and a refractive index detector (RID), using 0.6 mL/min of 0.005 M sulfuric acid as a mobile phase. The standards for the HPLC analysis were glucose, galactose, and arabinose. Free monosaccharides were directly analysed in all samples previously filtered through a 0.22 μm pore size syringe filter (Scharlab). Total sugars were measured after acid hydrolysis of the samples according to the Laboratory Analytical Procedure [34] to hydrolyse all the oligosaccharides in monomeric sugars. Oligosaccharide fraction was calculated as the difference between total sugar content after acid hydrolysis and free monosaccharide content.

The total protein (TP) fraction released as peptides was determined by measuring the total nitrogen with a TOC-VCSN/TN analyser (Shimadzu) using KNO_3 as standard. It should be noticed that the nitrogen to protein conversion factor applied, 4.9, was the same as for the solid residue from the red macroalgae, despite it could have slightly varied due to protein hydrolysis by subcritical water treatment [5]. Free amino acids (AA) were measured by using the EZ:faast Phenomenex procedure and derivatized samples were analysed by gas chromatography (Hewlett-Packard, 6890 series) with an EZ:faast AAA LC-integrated column and FID detector, using norleucine as internal standard.

Total phenolic compounds (TPC), reducing capacity (RC) and browning degree (BD). TPC was determined according to Folin-Ciocalteu procedure [35] using gallic acid as standard. RC was assessed by the ferric reducing ability of plasma method (FRAP) according to the Benzie and Strain procedure [36]. Results were expressed in mmol of Fe^{2+} /L. BD was determined by UV-Vis spectrophotometry at

420 ± 0.4 nm using a Hitachi U-2000 UV/Vis spectrophotometer.

Total organic carbon (TOC), total solids (TS) and pH. TOC was measured with a TOC-VCSN/TN analyser (Shimadzu) by difference of estimated total and inorganic carbon, using $\text{C}_6\text{H}_{14}(\text{COOK})(\text{COOH})$, NaHCO_3 and Na_2CO_3 as standards. TS was measured by drying the samples (feed, permeates and retentates) at 105 $^\circ\text{C}$ to remove water until constant weight. TS was estimated as the ratio between the residual weight of the dry sample after removing water by evaporation and the weight of the wet sample. The pH was measured using a Crison 52-08 pH electrode, with an analytical error of ± 0.01 pH units.

Particle size distribution was measured by laser diffraction by using a Malvern Mastersizer 2000 particle size analyser (Malvern Instruments Ltd., UK) with a measuring range from 0.02 to 2000 μm . Three replicates of five measurements were performed for each sample. The volume-weighted mean particle diameter, D [4,3], was estimated as:

$$D[4,3] = \frac{\sum n_i D_i^4}{\sum n_i D_i^3} \quad (7)$$

where n_i is the number of particles in size class i with a D_i diameter.

2.7. Process parameters

Results were expressed as percentage variation of the permeate and retentate content regarding the initial content in the SWH used as feed. The retention degree of the different SWH compounds, R_i , at the end of each filtration experiment was estimated as follows:

$$R_i(\%) = \left(1 - \frac{C_{i(p)}}{C_{i(0)}}\right) \cdot 100 \quad (8)$$

and the transmission coefficients, Tr_i , were determined as:

$$Tr_i(\%) = \frac{C_{i(p)}}{C_{i(r)}} \cdot 100 \quad (9)$$

where C_i (mg/L) is the compound concentration, and subscripts p, r and 0 refer to the permeate, retentate and SWH solution (initial), respectively. Concentrations in the retentate were also calculated by mass balances, with errors less than 2.8% for all analysed compounds.

The selectivity, α , of ultrafiltration between TP fraction and oligosaccharides (OS) was estimated as:

$$\alpha = \frac{Tr_{TP}}{Tr_j} \quad (10)$$

where subscript j refers to glucans (glOS), galactans (gOS), arabinans (aOS), and total oligosaccharides (total OS). The selectivity between TP and TPC was also estimated as the ratio of their transmission coefficients.

The TP purity index, PI, regarding total solids was calculated as follows:

$$PI(\%) = \frac{C_{TP}}{C_{TS}} \cdot 100 \quad (11)$$

2.8. Statistical analysis

Each experiment was performed at least twice and the feed solution, permeates and retentates collected throughout ultrafiltration, final permeate, and final retentate were analysed in triplicate. The results were expressed as mean \pm standard deviation in order to evaluate the dispersion degree of all experiment with the same operation conditions and to validate the data. The Fisher's least significant differences (LSD) method at p -value ≤ 0.05 was applied to confirm significant differences. A Statgraphics Centurion 18 software package (Statistical graph Co., Rockville, MD, USA) was used for statistical processing of the experimental data.

3. Results and discussion

3.1. Subcritical water hydrolysate

Chemical composition of the SWH used as feed for UF fractionation is collected in Table 1. TOC accounted for 2093 ± 40 mg/L. Most of the organic carbon comes from subcritical water hydrolysis of the macroalgal polysaccharide fraction with 551 ± 10 , 839 ± 9 , 131 ± 7 mg/L for

Table 1

Chemical composition of the subcritical water hydrolysate used as feed solution in the ultrafiltration experiments. The value of the purity index towards TP (PI) was estimated by Eq. (11).

	COMPOSITION
TOC (mg/L)	2093 ± 40
Total solids (TS, g/L)	6.1 ± 0.6
Glucans (glOS, mg/L)	551 ± 10
Galactans (gOS, mg/L)	839 ± 9
Arabinans (aOS, mg/L)	131 ± 7
Total peptides (TP, mg/L)	1761 ± 5
Free amino acids (AA, mg/L)	64.5 ± 0.8
Total phenolic compounds (TPC, mg/L)	219 ± 10
Reducing capacity (RC, mmol Fe^{2+} /L)	3.6 ± 0.4
PI in TP (%)	28.9
Volumic mass at 20 °C (g/L)	999.852 ± 0.001
Volumic mass at 50 °C (g/L)	988.001 ± 0.001
D [4,3] (dissolved matter, nm)	69.1 ± 0.1
pH	5.98 ± 0.06

glucans, galactans and arabinans, respectively. Total sugar content in the hydrolysate comes mainly from oligomer, as no free mono-saccharides have been detected. Moreover, the TP fraction in the SWH was 1761 ± 5 mg/L with a small amount of free amino acids, 64.5 ± 0.8 mg AA/L. The free amino acid profile has been collected in Table 1S. The main free amino acids in the hydrolysate were alanine (16.2 wt%), glycine (15.5 wt%), serine (7.1 wt%) and aspartic acid (32.0 wt%). The TPC was determined to be 219 ± 10 mg/L with a reducing capacity of 3.6 ± 0.4 mmol Fe^{2+} /L.

This characterization indicates that the SWH from the macroalgal solid residue is a complex mixture of different polymeric compounds with a potential foulant effect. In addition, the particle size distribution of the SWH in Fig. 3 shows the presence of colloidal and suspended matter with sizes above 0.2 μ m, which may also contribute to a severe reduction of the membrane permeability. Jarusutthirak et al. [37] reported that polysaccharide colloids were responsible for most fouling in UF membranes. To separate dissolved matter from colloidal matter, a sample of the SWH was centrifuged at 4000 rpm for 30 min. A liquid supernatant and a solid at the bottom of the cylinder were obtained. The particle size distribution of the supernatant, shown in Fig. 3, indicates that the size of the dissolved matter in the SWH ranged from 23 to 148 nm, with a rather low D [4,3] value of approximately 70 nm.

3.2. Ultrafiltration of SWH through a 5 kDa membrane: separation capacity and fouling

An efficient fractionation process requires high separation capacity and high permeate flux. Reversible and irreversible fouling creates additional resistances to permeate flux, especially when using fine-range UF membranes. An assessment of the separation efficiency and fouling of the 5 kDa tubular ceramic membrane has been carried out under different temperature and feed flow rate conditions: (a) SWH feed solution was ultrafiltered at 20 °C with a feed flow rate of 6.6 L/h ($Re = 1196$), (b) SWH feed solution was ultrafiltered at 20 °C with a feed flow rate of 11.2 L/h ($Re = 2040$) and (c) SWH feed solution was ultrafiltered at 50 °C with a feed flow rate of 11.2 L/h ($Re = 3622$).

The results of SWH filtration at $TMP = 1.1$ bar with the 5 kDa pore-sized membrane as a function of volume reduction (VRF) for the experiments at different temperature and feed flow rate (Q_F) are shown in Fig. 4. As a general trend, the permeation rate was much lower for the hydrolysate than for pure water. The pure water permeate flux, J_0 , at $TMP = 1.1$ bar was 46.9 ± 0.3 , 47.5 ± 0.5 and 49.3 ± 0.5 $L/m^2 h$ using 6.6 L water/h at 20 °C, 11.2 L water/h at 20 °C, and 11.2 L water/h at 50 °C, respectively. It is observed that the increase in Re caused by the increase in temperature and feed flow rate enhanced the pure water flux

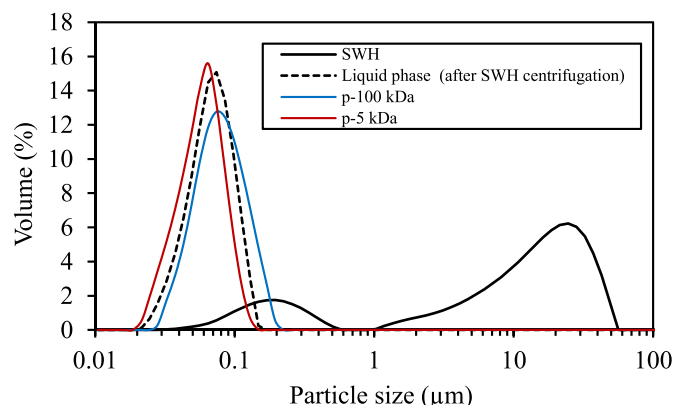


Fig. 3. Particle size distribution of the subcritical water hydrolysate (SWH), the liquid supernatant after centrifugation of the SWH, and of the permeates for the SWH filtration with 100 kDa (p-100 kDa) and 5 kDa (p-5 kDa) membranes. Ultrafiltration conditions: 20 °C, $TMP = 1.1$ bar, 11.2 L/h of feed flow rate and a final VRF of 4.1.

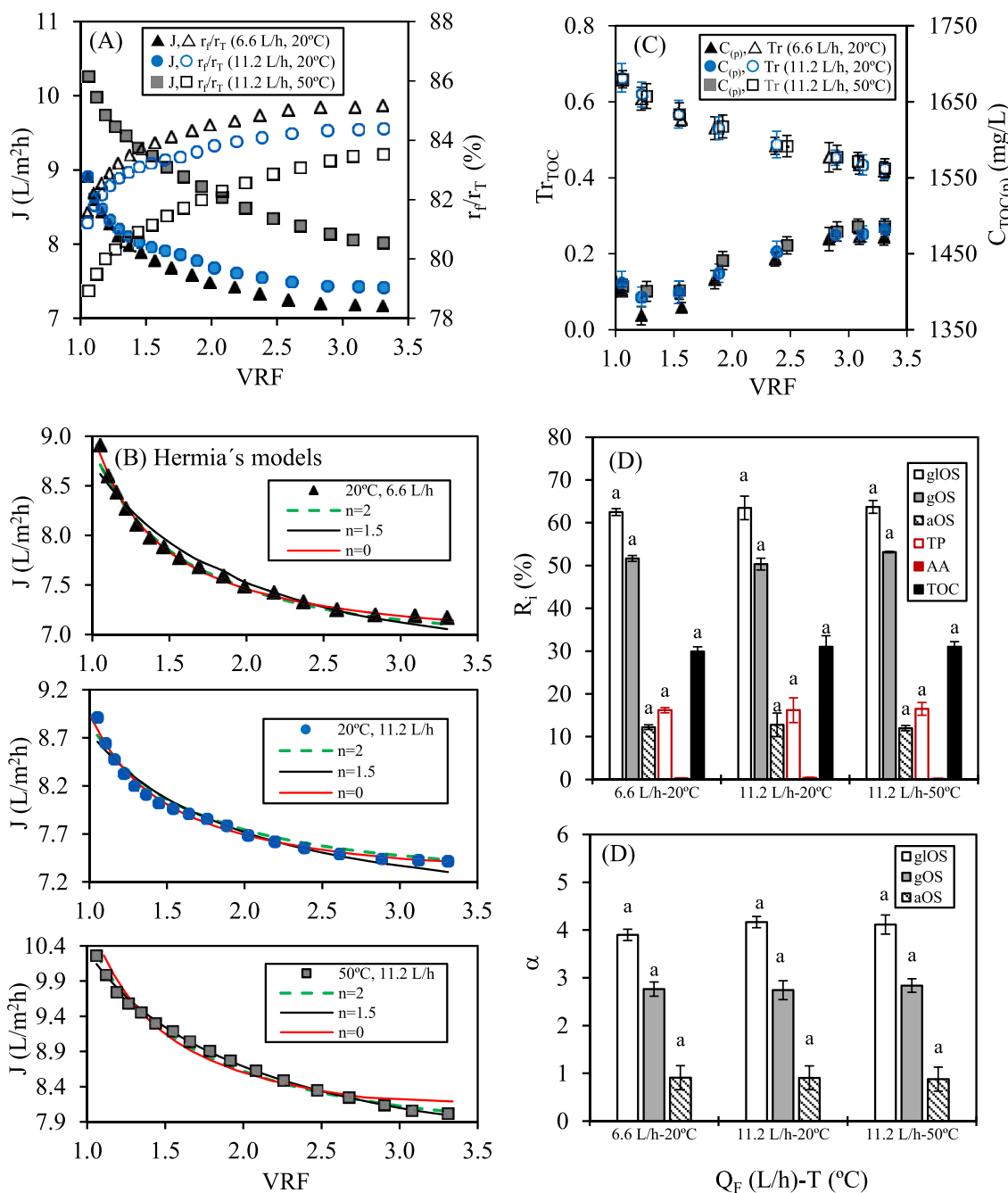


Fig. 4. Subcritical water hydrolysate filtration with a 5 kDa membrane at TMP = 1.1 bar, 20 °C or 50 °C, and a feed flow rate (Q_F) of 6.6 or 11.2 L/h. (A) Evolution of permeate flux (J) and fouling resistance contribution (r_f/r_T) with VRF. (B) Permeation flux modelled by Hermia's models (Eqs. (3)–(5)). (C) TOC transmission rate (Tr_{TOC} , by Eq. (9)) and concentrations in the permeate ($C_{TOC(p)}$) versus VRF along filtration. (D) Retention coefficients (R_i , by Eq. (8)), and selectivity (α , by Eq. (10)) at the end of filtration with a VRF = 3.3. Values with different letters for the same component indicate significant differences ($p \leq 0.05$).

through the 5 kDa membrane. Experimental data corresponding to permeate flux (J) and the contribution of fouling resistance to total resistance (r_f/r_T) are plotted against the VRF in Fig. 4A. The sharpest decrease in permeate flux was obtained at low VRF, with a flux loss (compared to J_0) at VRF = 1.3 of about 80% in the experiment at 50 °C and 83% in both experiments at 20 °C. This result might be explained by the fact that the permeate flux in the early stage of ultrafiltration was mainly controlled by the build-up of the polarization boundary layer [14,38,39], which seems to be more affected by the chemical composition and high concentration (~2000 mg TOC/L) of the red macroalgae hydrolysate than by the temperature, and unaffected by feed flow rate modification. In all experiments, the flux continued decreasing for VRFs

from 1.3 to 2.5–3 and then remained about constant until the end of the filtration.

It is also noted in Fig. 4A that, by increasing the feed flow rate from 6.6 L/h to 11.2 L/h, a slight variation in permeate flux around 3% for VRFs > 1.3 was obtained; however, by increasing the temperature from 20 °C to 50 °C, a considerable increase in permeate flux of more than 15% at the beginning of the filtration and about 10% at the end of filtration was achieved. The pseudo-steady state permeate flux resulted to be statistically higher at high temperature and high feed flow rate, with values close to 8.0 ± 0.1 L/m² h in the system at 50 °C, 7.4 ± 0.1 L/m² h in the system at 20 °C with high feed flow rate, and 7.1 ± 0.1 L/m² h in the systems at 20 °C with low feed flow rate. This result indicates

that for SWH feed solution, the permeate flux and the mass transfer coefficient were mainly affected by temperature and, to a lesser extent, by the feed flow rate. This favourable effect of temperature on the permeate flux due to lower permeate viscosity has also been confirmed in many studies [20,40–45], which is in accordance with the Hagen-Poiseuille equation.

Regarding fouling characterisation, the resistance-in-series model (Eq. (1)) has shown that the influence of r_m was considerably lower than the influence of r_f , indicating that concentration polarization and membrane fouling were the predominant contributions to the filtration resistance, accounting for more than 78% in all experiments, as can be seen in Fig. 4A. Comparison of the r_f/r_T profiles shows that SWH fouled the tubular 5 kDa membrane faster when using a low feed flow rate of 6.6 L/h at 20 °C than when using a feed flow rate of 11.2 L/h at the same temperature. The experiments carried out at 11.2 L/h showed that the fouling was faster the lower the temperature. In addition, the membrane fouling at the end of filtration was more severe at low temperature and feed flow rate.

Proper analysis and understanding of the membrane fouling mechanisms are essential to minimize fouling in order to improve the performance of SWH ultrafiltration. The Hermia's model was used to identify the fouling behaviour of the feed SWH at different temperatures and feed flow rates. Complete blocking (Eq. (4)), standard blocking (Eq. (5)), and cake layer formation (Eq. (6)) models were used to fit the experimental flux data shown in Fig. 4A. Experimental permeate flux data (symbols) and the predicted data (lines) by Eqs. (4)–(6) are presented in Fig. 4B. The results of fouling index k for each model (k_c , k_s and k_{cl}) and R^2 coefficients are listed in Table 2.


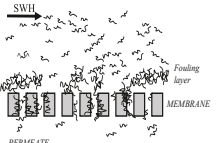
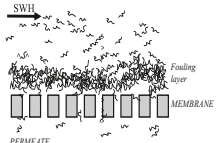
Considering the data in Fig. 4B and Table 2, the same predominant fouling mechanism was obtained for the SWH filtration at 20 °C using different feed flow rate. It is observed in Table 2 that the standard blocking and complete blocking models yielded poorer R^2 coefficients than cake layer model (0.9972 and 0.9947 for $Q_F = 6.6$ and 11.2 L/h, respectively), which provided the best fit to the experimental data (Fig. 4B) for both experiments at 20 °C. This result suggests that cake layer formation was the primarily responsible mechanism and fouling occurred predominantly on the membrane surface, resulting the permeate flux decline and the r_f increase controlled by the concentration polarization and the cake layer formation with low contribution of the pore blockage and pore constriction. The comparison of the coefficients k has been employed to evaluate the fouling potential for the same fouling mechanism at different feed flow rate and 20 °C. The k_c , k_s and k_{cl} values for a feed flow rate of 11.2 L/h were lower than for a feed flow rate of 6.6 L/h, suggesting that an increasing feed flow rate leads to a decrease in the cake layer resistance and in the blocking pore resistances, due to the increased mass transfer coefficient, the increased back-diffusion, and the reduced concentration polarization, which led to a reduction of solute accumulation over the membrane surface and the formation of a thinner and less compacted cake layer. However, the model that best fitted the experimental permeate flux data for SWH

filtration at 50 °C was the standard blocking model, with a R^2 coefficient of 0.9974. In addition, the comparison of the fouling index k shows that the k_{cl} of the cake layer resistance was lower for SWH filtration at 50 °C than for SWH filtration at 20 °C, thereby mitigating the cake layer formation. However, the index k of the blocking pore resistances (k_c and k_s) was notably higher at 50 °C than at 20 °C. Qi et al. [33] also observed the increase in pore blocking resistances when the temperature increased from 20 °C to 50 °C for oligodextran filtrations with ceramic membranes. This result implies that, at 50 °C, the permeate flux declined and the build-up of r_f were mainly controlled by the combined effect of standard and complete pore blocking resistances. Despite the fact that fouling was less severe at 50 °C, fouling occurred predominantly inside the pores with high impact on membrane lifetime. It is interesting to point out that the formation of a physically removable cake (or gelation layers) at the end of ultrafiltration was not detected in these experiments, even though the cake/gel layer formation resistance turned out the major contribution to the filtration resistance in experiments at 20 °C.

Fig. 4C and D shows the experimental data corresponding to the retention of the 5 kDa membrane. No significant temperature and feed flow rate effect on the organic matter transmission rate (T_{rTOC} by Eq. (9), Fig. 4C) and on retention coefficients (R_i by Eq. (8), Fig. 4D) was found ($p > 0.05$) from statistical analysis, even though these operating parameters affected the permeate flux owing to differences in fouling. However, the membrane retention depended on the VRF. As observed in Fig. 4C, the diffusive transport of organic solutes throughout the membrane was highly reduced along filtration, with the TOC transmission rate ranging from approximately 65% at the beginning of each filtration (VRF = 1.01) to 41% at the end of all filtrations (VRF = 3.3). In addition, the TOC concentration in the permeates increased slightly with VRF from 1370 to 1391 mg/L to 1465–1487 mg/L (~7% in each experiment), whereas the TOC concentration in the retentates increased 71–72% during ultrafiltration. A final retentate with about 3500 mg TOC/L (3527 ± 22, 3541 ± 35, and 3539 ± 31 mg TOC/L for experiments with $Q_F = 6.6$ L/h at 20 °C, $Q_F = 11.2$ L/h at 20 °C, and $Q_F = 11.2$ L/h at 50 °C, respectively) and the same total TOC retention (Fig. 4D) of about 30% were obtained in all experiments. It can be assumed that the loss of organic matter on top or inside the membrane by fouling effects was almost negligible due to the good agreement between the experimental TOC data and the mass-balance calculated TOC data in the retentate stream for each experiment along filtration, with errors lower than 1%. These results suggest that the organic matter transport throughout the 5 kDa TiO₂ tubular ceramic membrane during SWH filtration and retention coefficients seem to be primarily affected by the effect of increased retentate concentration with VRF more than by differences in fouling due to the operating temperature and feed flow rate modifications from 20 °C to 50 °C and from 6.6 to 11.2 L/h, respectively. Krawczyk et al. [25] reached similar conclusions for crossflow filtrations of hetero-polysaccharides with 10 kDa tubular α -Al₂O₃ and TiO₂ membranes in concentration mode. These authors explained that operating

Table 2

Determination coefficients (R^2) and foiling indexes (k_c , k_s and k_{cl}) of three fouling models for the filtration of the subcritical water hydrolysate (SWH) with a 5 kDa pore-sized membrane at different temperature (T) and feed flow rate (Q_F). CFV and Re refer to the crossflow velocity and the Reynolds number, respectively.

EXPERIMENTS									
T (°C)	Q_F (L/h)	CFV (m/s)	Re	Complete blocking (n = 2, Eq. (4))		Standard blocking (n = 1.5, Eq. (5))		Cake layer formation (n = 0, Eq. (6))	
				R^2	k_c (s ⁻¹)	R^2	k_s (s ^{-0.5} m ^{-0.5})	R^2	k_{cl} (s m ⁻²)
20	6.6	0.6	1196	0.9939	0.00011	0.9701	0.0068	0.9972	2.32·10 ⁷
20	11.2	1	2040	0.9899	0.00009	0.9657	0.0057	0.9947	1.96·10 ⁷
50	11.2	1	3622	0.9933	0.00011	0.9974	0.0084	0.9806	1.76·10 ⁷

temperature from 60 to 80 °C, pressure from 0.2 to 1.6 bar, and cross-flow velocity from 2 to 5 m/s affected the permeate flux and fouling, with no influence on membrane retention (96%) since the limiting operating parameter resulted to be the feed concentration. This effect was also observed by Giacobbo et al. [46], reaching the same polysaccharide retention, 99.3%, by modifying the operating pressure from 0.5 to 4 bar in the filtration of winery effluents with 7.6 kDa PES polymeric membranes.

Fig. 4D shows the results obtained for retention and selectivity at the end of filtration for the different chemical compounds determined in the SWH. Retention was negligible for free amino acids (AA), reaching values of 16% for peptides (TP), 63% for glucans (gLOS), 51% for galactans (gOS) and 13% for arabinans (aOS), hence indicating a notably higher retention for OS fraction than for TP fraction. These retention results suggest that glucans and galactans presented a higher molecular size distribution than the peptides and arabinans obtained by SWH. It was observed that the pH in retentates and permeates remained constant during the hydrolysate filtration, with values close to the pH of the feed solution (Table 1). It should be also considered that the membrane surface was negatively charged at the experimental pH and electrostatic interactions took place with the negatively charged functional group of glucans and galactans [10,11], which was probably a significant contribution to its decreased transport through the 5 kDa membrane. In addition, the 5 kDa membrane provided complete retention of colloidal and suspended matter, as can be inferred from the particle size distribution results in Fig. 3, where it can be observed that particles larger than 0.2 μm were not detected in the permeate stream. These colloids and suspended materials, together with the high OS fraction rejected by the membrane, were thus the main responsible for most of the r_f increase and permeate flux drop during SWH filtration. Regarding the separation

efficiency, Fig. 4D shows the selectivity of the 5 kDa membrane (α by Eq. (10)) for the separation of the TP fraction from the OS fraction. A high selectivity of the 5 kDa membrane for the TP separation from glucans and galactans was observed, but this membrane was inefficient for the separation of the TP fraction and arabinans ($\alpha = 1.0 \pm 0.1$). In any case, the arabinans fraction in the SWH accounted for less than 9 wt% of the total oligosaccharide fraction.

Since experimental conditions did not affect the retention and selectivity coefficients for the different chemical compounds, the effect of membrane pore size on SWH fractionation and process with sequential UF-stages were studied at the highest feed flow rate and the lowest temperature to avoid heating of the feed and to investigate the feasibility of the process at ambient temperature, as well as to mitigate the irreversible membrane fouling during ultrafiltration. The final VRF was increased from 3.3 to 4.1 due to its impact on the fractionation process.

3.3. Effect of the membrane pore size on SWH ultrafiltration

The following step was focused on analysing the effect of the membrane pore size on the permeate flux and on the separation efficiency of peptides from the different oligosaccharides and other organic compounds in the SWH. An evaluation of the purity index towards the peptide fraction was performed to assess the degree of purification achieved in each filtration.

Experimental data for SWH filtration at 20 °C, TMP = 1.1 bar, and $Q_F = 11.2$ L/h with different pore-sized membranes from 5 to 100 kDa are presented in Fig. 5. The results of filtration resistances (r_T , r_m , and r_f , m^{-1}), retention coefficients at the end of filtration with a VRF = 4.1 (R, %), purity index in TP (PI, %), D [4,3] value for final permeates, and the pH values are listed in Table 3.

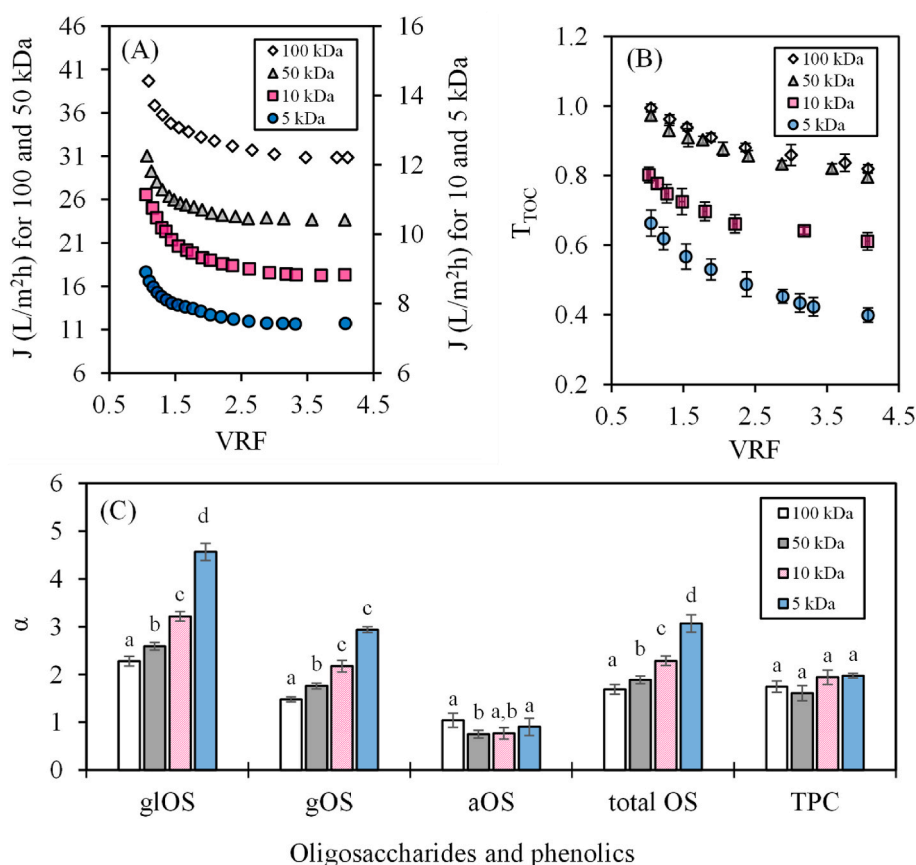


Fig. 5. Effect of the membrane pore size (5–100 kDa) on the subcritical water hydrolysate filtration at 20 °C, TMP = 1.1 bar and 11.2 L/h of feed flow rate. (A) Evolution of permeate flux (J) with VRF. (B) TOC transmission rate (T_{TOC} , by Eq. 9) versus VRF along filtration. (C) Selectivity (α , by Eq. 10) towards peptide fraction at the end of filtration with a VRF = 4.1. Values with different letters for the same component indicate significant differences ($p \leq 0.05$).

Table 3

Experimental parameters for the filtration of the subcritical water hydrolysate by using the different membranes at 20 °C, TMP = 1.1 bar, and 11.2 L/h of feed flow rate. Values with different letters for the same component indicate significant differences (LSD, $p \leq 0.05$).

PARAMETERS	100 kDa	50 kDa	10 kDa	5 kDa
J (L/m ² h)	39.7–30.9	31.0–23.8	11.1–8.6	8.9–7.4
VRF	1.05–4.10	1.05–4.10	1.05–4.10	1.05–4.10
r_T (10 ¹³ m ⁻¹)	0.94–1.20	1.16–1.52	3.13–4.08	4.17–5.00
r_m (10 ¹³ m ⁻¹)	0.20	0.25	0.64	0.78
r_f (10 ¹³ m ⁻¹)	0.74–1.00	0.91–1.28	2.59–3.43	3.38–4.22
r_f/r_T (%)	78.7–83.4	78.8–83.8	79.4–84.2	81.2–84.4
PI in TP (%)	30.5 ± 0.8 ^a	38.9 ± 0.8 ^b	41 ± 1 ^c	45 ± 1 ^d
R _{TOC} (%)	6.7 ± 0.5 ^a	7.9 ± 0.5 ^b	14 ± 2 ^c	31 ± 1 ^d
R _{TS} (%)	10.2 ± 0.8 ^a	38.0 ± 0.8 ^b	40.8 ± 0.9 ^c	45.7 ± 0.8 ^d
R _{TP} (%)	5.1 ± 0.9 ^a	16.5 ± 0.6 ^b	16.0 ± 0.7 ^b	15.9 ± 0.9 ^b
R _{AA} (%)	0.3 ± 0.3 ^a	0.1 ± 0.2 ^a	0.2 ± 0.3 ^a	0.1 ± 0.1 ^a
R _{OS} (%)	20.8 ± 0.8 ^a	35 ± 2 ^b	41 ± 1 ^c	55 ± 2 ^d
R _{glOS} (%)	30.4 ± 0.7 ^a	47.5 ± 0.7 ^b	54 ± 1 ^c	64 ± 1 ^d
R _{gOS} (%)	16.5 ± 0.9 ^a	35 ± 1 ^b	41 ± 1 ^c	50.8 ± 0.9 ^d
R _{aOS} (%)	6.0 ± 1.0 ^a	8 ± 2 ^a	8 ± 2 ^a	13 ± 2 ^b
R _{TPC} (%)	21.7 ± 0.2 ^a	31.9 ± 0.3 ^b	37.2 ± 0.3 ^c	38.0 ± 0.3 ^d
R _{RC} (%)	23 ± 2 ^a	35 ± 1 ^b	41 ± 3 ^c	57 ± 2 ^d
R _{BD} (%)	17.4 ± 0.8 ^a	36.0 ± 0.5 ^b	41.7 ± 0.5 ^c	56.2 ± 0.8 ^d
pH _(p)	6.1 ± 0.2 ^a	6.1 ± 0.2 ^a	5.8 ± 0.1 ^a	5.9 ± 0.1 ^a
pH _(r)	6.0 ± 0.1 ^a	5.9 ± 0.2 ^a	6.2 ± 0.2 ^a	6.0 ± 0.2 ^a
D [4,3] _(p) (nm)	86.0 ± 0.3	82.2 ± 0.3	69.0 ± 0.2	58.0 ± 0.2

J: permeate flux; r_T , r_m and r_f : filtration resistances estimated by Eq. (1); PI: purity index towards TP in final permeate estimated by Eq. (11); R: retention coefficients at the end of filtration estimated by Eq. (8); pH_(p): average permeate pH; pH_(r): average retentate pH; D [4,3]_(p): the mean volume-weighted particle size in final permeate. TOC: total organic carbon, TS: total solids, TP: total peptide fraction, AA: total free amino acids, OS: total oligosaccharides, glOS: glucans, gOS: galactans, aOS: arabinans, TPC: total phenolics, RC: reducing capacity, BD: browning degree.

3.3.1. Total permeation flux and fouling

The permeate flux clearly increased by increasing membrane pore size from 5 to 100 kDa as can be observed in Fig. 5A. The profile of the permeate flux loss with VRF was similar for all the membranes. A considerably high flux loss, with regard to pure water, was observed at the beginning of the filtration, a continuous decrease of the flux up to VRF 2–2.5 and then the flux remained constant at around 31 L/m² h for the membrane with the highest cut-off size and slightly above 7 L/m² h for the membranes with the lowest cut-off size. The fouling behaviour was similar for all membranes. It is observed in Table 3 that r_f (> r_m) was the predominant contribution to r_T and flux loss, indicating that concentration polarization and membrane fouling were the predominant contributions to the filtration resistance. However, the decrease in r_f from 3.38 to 4.22 · 10¹³ m⁻¹ to 0.74–1.00 · 10¹³ m⁻¹ with increasing membrane pore size from 5 to 100 kDa can be explained as a result of a marked decrease in membrane retention of all the SWH components (Table 3), which led to the reduction of the concentration polarization layer development and solute deposition onto the membrane surface.

3.3.2. Selectivity of ultrafiltration

As observed in Fig. 5B, the organic matter transport throughout the membrane depended on the membrane pore size and on the VRF. At each VRF, the mass transfer rate of organic solutes across the membrane was considerably lower for 5 kDa cut-off size than for 10, 50 and 100 kDa. Moreover, the organic matter transmission rate ($Tr_{(TOC)}$) ranged from values around 99%–80% along filtration with the 100 and 50 kDa cut-off sizes, indicating that these pore sizes have turned out to be excessively large for the molecular weight of the main SWH compounds. These results were also observed by comparison of the membrane selectivity (α) in Fig. 5C and the purity index (IP) towards TP in Table 3. Separation between TP and total OS was considerably reduced from 3 to 1.7 when the membrane pore size increased from 5 kDa to 100 kDa,

leading to a final permeate with a low TP purity index close to 30%. However, the 100 kDa cut-off size provided a colloid-free permeate with a range size of dissolved matter between 25 nm and 200 nm, as shown by the particle size distribution results in Fig. 3. A similar permeate particle size distribution profile was obtained for all membranes, with hardly any variation in the dissolved matter size range and D [4,3] values of the same order of magnitude as can be seen in Table 3. This result justified that the 100 kDa cut-off membrane was enough to retain all colloidal and suspended matter from the SWH with a particle size above 0.2 μ m.

It is interesting to point out that the highest selectivity of all membranes was found for the separation of TP from glucans and galactans, but the selectivity for arabinans and TPC resulted to be low and independent on the membrane pore size. Thus, 5 kDa cut-off membrane was still a large membrane cut-off size for obtaining an efficient separation of the TP fraction, as it was already found in the preliminary studies with the 5 kDa membrane (Section 3.2).

3.3.3. Peptide fraction

A more detailed comparison of retention coefficients (Table 3) for different membranes and compounds shows that TP fraction retention (R_{TP}) was one of the lowest for all the tested membranes, even when using the 5 kDa cut-off size. Retention was negligible for free amino acids and a slight increase in retention of peptides was just observed between 100 kDa (5%) and 50 kDa (16%) membranes with no further increase of retention for lower MWCO membranes. Yu et al. [15] observed a total protein retention with a 10 kDa membrane in the filtration of fresh rapeseed extracts obtained by grinding and mixing with water. They explained that the high levels of protein retention were due to the composition of the raw material, mainly constituted of high molecular weight globulins (300 kDa) and albumin proteins (12–14 kDa). Saidi et al. [14] found total retention of the peptide fraction with molecular weight distribution higher than 7 kDa from fish protein hydrolysates by using an 8 kDa cut-off ceramic membrane. Hence, the low retention obtained for the protein fraction in this work can be explained considering that the extraction/hydrolysis under subcritical conditions has provided the presence of low molecular weight peptides as the main TP species in the SWH. In addition, these results suggest that about 5% of the TP fraction was larger than 100 kDa, but the largest fraction of TP in the SWH was peptides smaller than 5 kDa with a small amount of free amino acids.

3.3.4. Oligosaccharide fraction

OS fraction showed the highest rejection from approximately 21% for the 100 kDa membrane to 55% for the 5 kDa membrane as can be observed in Table 3. Glucans were the most retained components, $R_{glOS} = 30\%$ –64%, followed by galactans, $R_{gOS} = 16\%$ –51%, and finally arabinans were poorly retained with all the tested membranes, $R_{aOS} = 6\%$ –13%. Hence, the relation between the membrane pore size and retention was observed, although no significant differences were found between 100 and 10 kDa cut-off sizes for arabinans. From these results it can be concluded that the glucans and galactans presented higher molecular size distribution than the peptides obtained in the extraction process under subcritical conditions, however the largest fraction of arabinans (~87%) in SWH was smaller than 5 kDa, although as previously described, the arabinans fraction represented only the 9% of the total OS fraction.

3.3.5. Total phenolic compounds (TPC), browning degree (BD) and reducing capacity (RC)

The retention of TPC (R_{TPC}) showed the same trend as browning degree (R_{BD}) and reducing capacity (R_{RC}). An increase in R_{TPC} from 22% to 38%, in R_B from 17% to 56% and in R_{RC} from 23% to 57% was observed with the reduction of the membrane pore size from 100 to 5 kDa, as shown in Table 3. The correlation between the retention of TPC and antioxidant capacity has also been confirmed in several studies. Tsihranska et al. [47] found that by decreasing the membrane pore size

from 900 Da to 300 Da for propolis filtration, the antioxidant capacity of the retentate increased, at the same time that a decrease was observed in the permeate stream due to an increase in the retention of total polyphenols and flavonoids. Arend et al. [48] indicated that the retention of total phenolics, total monomeric anthocyanins and antioxidant activity increased with the volume reduction factor during nanofiltration of strawberry juices in concentration mode. They found that the antioxidant activity was adequately correlated with total phenolic content and with the concentration of the major anthocyanin detected in the juice, pelargonidin-3-O-glycoside. Additionally, Díaz-Reinoso et al. [49] obtained high retention for phenolics (80–90%) and antioxidant activity in filtrations of distilled white grape pomace with 1 kDa ceramic membrane.

However, the comparison of retention results for the lowest membrane pore sizes shows a slight variation in R_{TPC} between 37 and 38% and a large increase in R_{RC} between 41 and 57%, suggesting that browning products also present a strong correlation with the reducing power. Melanoidins, with high antioxidant power, are compounds formed as a consequence of Maillard and caramelization reactions at high temperatures between carbonyl and amine groups from reducing sugars and amino acids, respectively [50,51]. According to a previous work [5], Maillard reaction products were the main responsible for browning degree on the SWHs of the macroalgae solid residue. It was also observed that TPC and Maillard reaction products of the SWH showed stronger correlations with reducing capacity than other hydrolysate components, such as peptides and free amino acids, as it has also been seen in this work. It can be concluded that, by using 5 kDa membrane, the largest fraction of peptides, phenolics and Maillard reaction products were collected in the permeate, which preserved about 40% of the starting reducing capacity of the SWH.

3.4. Sequential ultrafiltration integrated with freeze-drying

Based on the separation results of the 5 and 100 kDa membranes, a process with sequential filtrations has been designed to study its suitability to improve the SWH fractionation.

To separate and concentrate OS and TP fractions, a combined process with sequential filtration stages and a subsequent freeze-drying stage was examined (Fig. 2). All filtrations were carried out at 20 °C to avoid heating and additional costs, $TMP = 1.1$ bar and $Q_F = 11.2$ L/h. The VRF was 4.1 for filtrations with 100 kDa and 5 kDa membranes and 2.1 for filtration with 1 kDa membrane. A good reproducibility of the multi-stage filtration process was observed, due to the fact that no statistically significant differences ($p \leq 0.05$) were found between replicate stages in Cycle A (UFs with 100 and 5 kDa membranes) and Cycle B (UFs with 100, 5, and 1 kDa membranes). A constant permeate flux of about 18 and 11 L/m² h was obtained during filtrations with 5 kDa and 1 kDa membranes, respectively. Some of the experimental results are shown in Table 4 and Fig. 6.

The retention coefficients for each filtration stage are shown in Fig. 6A. By a multi-stage filtration process, most of total solid (TS) content was removed, remaining 89.8%, 49.4% and 27.1% of initial TS in the permeate after filtration through the 100, 5 and 1 kDa membrane, respectively. In the first filtration stage with an ultimate VRF = 4.1, the retention of the 100 kDa membrane for the different SWH components was statistically similar to that shown in Table 3. A good clarification of the feed hydrolysate was obtained since 100 kDa membrane provided total retention of colloidal and suspended materials and a slightly higher retention for OS fraction (20.6%) than for TP fraction (5.1%). TPC and BD were also poorly retained by the 100 kDa membrane, at around 22% and 17% respectively. Similar retention value was obtained for RC, 23%. As discussed above, this result may be due to the fact that TPC and browning compounds were probably the main SWH compounds with reducing capacity.

In the second filtration stage with the 5 kDa membrane at VRF = 4.1, when passing the 100 kDa permeate stream (p1) through the 5 kDa

Table 4

Composition of permeate (p1, p2 and p3), retentate of the 1 kDa filtration (r3) and dry solid obtained in Cycle A (S_A from p2) and in Cycle B (S_B from p3) for the fractionation process shown in Fig. 2.

COMPOUNDS, MASS OF SOLIDS, RF AND PI VALUE	CYCLE A (100 and 5 kDa)			CYCLE B (100, 5, and 1 kDa)		
	C_{p1} (mg/L)	C_{p2} (mg/L)	w_{SA} (mg/ mg dry solid)	C_{p3} (mg/L)	w_{SB} (mg/ mg dry solid)	C_{r3} (mg/L)
Total solids (TS)	5477.8 ± 0.2	3013.4 ± 0.1	–	1653.4 ± 0.1	–	4524.3 ± 0.3
Total peptides (TP)	1671.2 ± 0.1	1459.9 ± 0.5	0.487 ± 0.002	1170.5 ± 0.2	0.712 ± 0.002	1780.3 ± 0.6
Glucans (gIOS)	382.4 ± 0.4	197.6 ± 0.1	0.07 ± 0.04	54.5 ± 0.1	0.033 ± 0.008	354.9 ± 0.3
Galactans (gOS)	700.6 ± 0.5	434.8 ± 0.1	0.146 ± 0.003	168.1 ± 0.2	0.102 ± 0.002	731.1 ± 0.3
Arabinans (aOS)	123.1 ± 0.2	114.6 ± 0.2	0.038 ± 0.009	51.1 ± 0.2	0.031 ± 0.005	185.2 ± 0.4
Total phenolic compounds (TPC)	171.5 ± 0.5	133.1 ± 0.5	0.045 ± 0.003	77.4 ± 0.3	0.047 ± 0.002	195.0 ± 0.4
RF_{TP} (wt.%)	72 ± 1	87.4 ± 0.6	–	42.2 ± 0.6	–	57.8 ± 0.3
RF_{OS} (wt.%)	59.9 ± 0.5	46.9 ± 0.4	–	19.3 ± 0.4	–	80.6 ± 0.5
Mass of S_A and S_B (mg) ^a	–	–	3404 ± 8	–	985 ± 2	–
PI (wt.%)	30.5 ± 0.2	48.4 ± 0.7	48.7 ± 0.2	70.8 ± 0.5	71.2 ± 0.1	39.3 ± 0.8

C_p : concentrations in the permeate; w: compound mass fraction in the dry solid; RF: recovery factors expressed as percentage variation of the compound mass in the permeate or retentate per the initial compound mass in the feed of each UF stage; PI: TP purity index in final permeates estimated by Eq. (11) and for the dry solid.

^a Mass of S_A and S_B refers to the mass of dry solid per 2 L of SWH (Fig. 2).

membrane, a significant increase in retention was observed for all the compounds analysed, but retention was more intense for glucans (64.0 ± 1% of the initial gIOS), galactans (48.2 ± 0.5% of the initial gOS), and coloured compounds (51.4 ± 0.7% of the initial BD). This browning reduction in the permeate and browning intensification in the retentate can also be visually observed in the photographs included in Fig. 2. However, the TP fraction was not greatly affected by this filtration stage, since just 17.1 ± 0.5% was retained after filtration through 100 and 5 kDa membranes. As expected, the retention results in Cycle A and the purity index towards TP of the final permeate p2 (Table 4) matched those obtained in the SWH single-stage filtration with the 5 kDa membrane (Table 3 and Fig. 5C).

When passing the permeate stream from 5 kDa membrane (p_2) through the 1 kDa membrane (Cycle B in Fig. 2), OS retention still continued to increase significantly, obtaining a total retention of 89.7 ± 0.8% for glucans, 80.0 ± 1.0% for galactans and 61.0 ± 2.0% for arabinans, as can be seen in Fig. 6A. It can be also observed a considerable increase in retention of the TPC, BD and RC, more than 64%, 81%, and 87% of the initial SWH content, respectively. Nevertheless, TP retention coefficient stayed small, approximately 33.5 ± 0.7% respect to the initial SWH content. No significant retention of free AA fraction was observed in the filtration with the 5 and 1 kDa membranes, as shown in Fig. 6B. This means that the filtration with 1 kDa cut-off size was an efficient fractionation stage for the separation of the TP fraction from most of the TPC fraction, browning colour and total OS fraction, including arabinans.

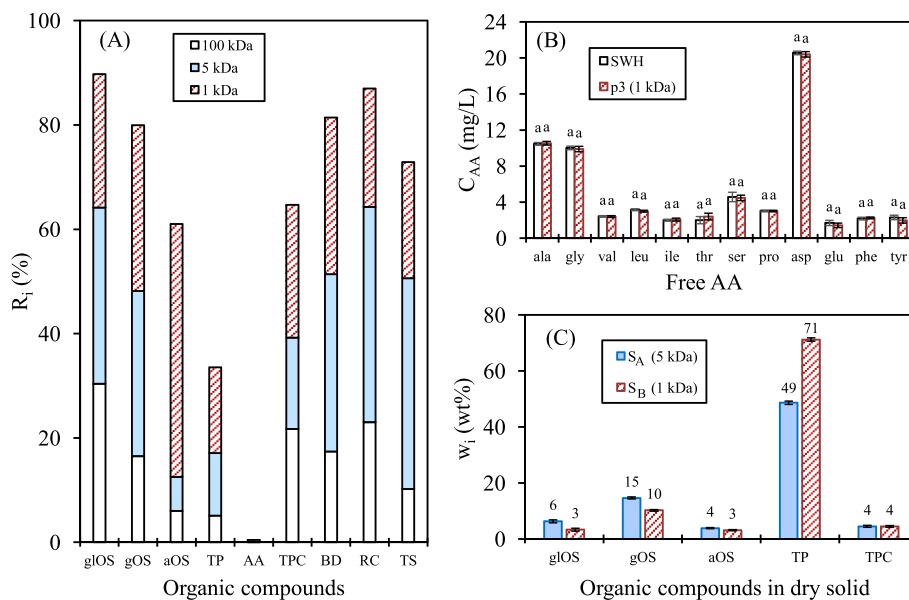


Fig. 6. Experimental results for the fractionation process shown in Fig. 2. (A) Retention coefficients (R_i , by Eq. (8)) at the end of each filtration stage. (B) Concentration of free amino acids (AA) in the subcritical water hydrolysate (SWH) and in the final permeate obtained after filtration with the 1 kDa membrane (p3). (C) Composition of the dry solid (w_i , g component/100 g dry solid) obtained in Cycle A (S_A) and in Cycle B (S_B).

The composition results of permeates p2 (from the 5 kDa membrane) and p3 (from the 1 kDa membrane), presented in Table 4, show that more than 92% of the total solids in p3 were TP, OS, and TPC with a TP purity index (PI by Eq. (11)) close to 71%, while in p2, TP, OS, and TPC only accounted for the 78% of the total solids and the TP purity index was 48%.

Final permeates p2 and p3 were freeze dried. Lyophilization showed a high recovery yield of 98.7% and 98.9% for p2 (Cycle A) and p3 (Cycle B), respectively. The composition of the dry solids was summarised in Table 4 and Fig. 6C. A good agreement between permeate composition and dry solid composition has been obtained. The main component was TP fraction in both solids. According to Fig. 6C, Cycle B was more efficient than Cycle A, since the dry solid from permeate p3, obtained from the 1 kDa membrane, was much rich in peptides (71 wt%) than the permeate p2 obtained from the 5 kDa membrane (48 wt%).

In addition, the recovery factor of TP in mass (RF_{TP} in Table 4) was also calculated for each filtration stage. These mass results corroborate that loss of TP mass in the retentates was low in the first and in the second filtration, but the 1 kDa membrane removed more than 50% of the feed TP mass. Thus, a retentate r3 with 39% of peptides in the range of 1 and 5 kDa was achieved, while a solid S_B with more than 70% of peptides with a molecular weight size below 1 kDa was obtained. The molecular weights of peptides have a high impact on their bioactive properties such as antioxidant, antimicrobial, or antihyperglycemic among others. The fractionation of peptides resulting from protein hydrolysis has become a usual practice to investigate the properties of the final hydrolysed products, such as the solid S_B and the retentate r3 (Table 4). Further work is needed to evaluate the different functional properties of the fractionated peptides obtained in this work.

4. Conclusions

Subcritical water hydrolysate from red macroalgae residue was a source of valuable bioactive compounds, which make it an excellent substrate for fractionation and concentration by means of membrane technology separation. Crossflow ultrafiltration with ceramic membranes has proven to be a suitable separation technology to isolate the oligosaccharides and peptide fraction. By decreasing the membrane pore size from 100 to 5 kDa, higher retentions were achieved for glucans, galactans and phenolics. However, the 5 kDa membrane was ineffective

for the separation of the peptides and arabinans, both of which were mostly collected in the permeate stream. The increase in feed flow rate from 6.6 to 11.2 L/h and temperature from 20 to 50 °C played an important role in hydraulic fouling and in the loss of permeate flux for the 5 kDa membrane; however, these operating parameters did not influence the retention of the membrane. By using sequential ultrafiltration steps with different membranes cut-off sized membranes, it was possible to fractionate and concentrate the oligosaccharides and peptides from the hydrolysate. A sum of retentates with more than 90 wt% of the SWH total oligosaccharide fraction and a final permeate with a purity index towards peptides close to 71 wt% were collected after sequential ultrafiltration by using 100, 5 and 1 kDa membranes. Lyophilisation was an effective technique for permeate treatment due to the low losses of total solids. A dry solid, rich in peptides (71 wt%), with a good cake appearance that could be used in different applications, was obtained.

Author statement

E. Trigueros: Investigation, Data curation, Writing – original draft.

M. T. Sanz: Project administration, Methodology, Supervision, Writing -review & editing.

S. Beltrán: Project administration, Funding acquisition, Supervision, Writing -review & editing.

María Olga Ruiz*: Conceptualization, Methodology, Data curation, Supervision, Writing -review & editing.

Declaration of competing interest

The authors declare that they have no known competing financial interests or personal relationships that could have appeared to influence the work reported in this paper.

Data availability

I have shared the link to my data at the attach file step

Acknowledgments

The authors gratefully acknowledge the financial support provided

by the Agencia Estatal de Investigación [grant number PID2019-104950RB-I00/AEI/10.13039/501100011033] and by the Junta de Castilla y León (JCyL) and the European Regional Development

Fund (ERF) [grant number BU050P20]. E. Trigueros predoctoral contract was funded by the JCyL and the European Social Fund (ESF) by ORDEN EDU/574/2018.

Appendix A. Supplementary data

Supplementary data to this article can be found online at <https://doi.org/10.1016/j.memsci.2022.120822>.

NOMENCLATURE

List of symbols

AA	total free amino acids
aOS	arabinans
BD	browning degree
C	compound concentration (mg L^{-1})
$D[4,3]$	the volume-weighted mean particle diameter estimated by Eq. (7) (μm)
glOS	glucans
gOS	galactans
J	permeate flux ($\text{L m}^{-2}\cdot\text{h}^{-1}$)
J^*	critical flux parameter defined in Eq. (3) ($\text{L m}^{-2}\cdot\text{h}^{-1}$)
J_0	pure water permeate flux ($\text{L m}^{-2}\cdot\text{h}^{-1}$)
k	parameter of Eq. 3
k_c	fouling index of Eq. (4) (s^{-1})
k_{cl}	fouling index of Eq. (6) (s m^{-2})
k_s	fouling index of Eq. (5) ($\text{s}^{-0.5}\text{m}^{-0.5}$)
n	parameter of Eq. 3
OS	oligosaccharides
PI	purity index towards TP in final permeates estimated by Eq. 11
Q_F	feed flow rate (L h^{-1})
r_f	fouling resistance of Eq. (1) (m^{-1})
r_m	membrane hydraulic resistance of Eq. (1) (m^{-1})
r_T	total filtration resistance of Eq. (1) (m^{-1})
R	degree of retention estimated by Eq. (8) (%)
Re	Reynolds number
R^2	determination coefficient
RC	reducing capacity
SW	subcritical water
SWH	subcritical water hydrolysate
T	temperature ($^{\circ}\text{C}$)
TOC	total organic carbon
TP	total protein fraction
TPC	total phenolic compounds
TPM	transmembrane pressure (Pa)
Tr	transmission coefficient estimated by Eq. 9
TS	total solids
V	volume (L)
VRF	volume reduction factor
w	mass of compound per unit of mass of dry solid (g g^{-1})

Greek symbols

α	selectivity estimated by Eq. 10
μ	viscosity of the permeate (Pa·s)

Subscripts

0	subcritical water hydrolysate used as feed solution
i	each group of hydrolysate compounds
j	total oligosaccharides and each oligosaccharide group
p	permeate stream
r	retentate stream

References

- [1] P. Guerrero, A. Etxabide, I. Leceta, M. Peñalba, K. de la Caba, Extraction of agar from *Gelidium sesquipedale* (Rhodophyta) and surface characterization of agar based films, *Carbohydr. Polym.* 99 (2014) 491–498, <https://doi.org/10.1016/j.carbpol.2013.08.049>.
- [2] E. Murano, Chemical structure and quality of agars from *Gracilaria*, *J. Appl. Phycol.* 7 (1995) 245–254, <https://doi.org/10.1007/BF00003999>.
- [3] R. Carmona, J.J. Vergara, M. Lahaye, F.X. Niell, Light quality affects morphology and polysaccharide yield and composition of *Gelidium sesquipedale* (Rhodophyceae), *J. Appl. Phycol.* 10 (1998) 323–331, <https://doi.org/10.1023/A:1008042904972>.
- [4] E. Trigueros, M.T. Sanz, A. Filipigh, S. Beltrán, P. Riaño, Enzymatic hydrolysis of the industrial solid residue of red seaweed after agar extraction: extracts characterization and modelling, *Food Bioprod. Process.* 126 (2021) 356–366, <https://doi.org/10.1016/j.fbp.2021.01.014>.
- [5] E. Trigueros, M.T. Sanz, P. Alonso-Riño, S. Beltrán, C. Ramos, R. Melgosa, Recovery of the protein fraction with high antioxidant activity from red seaweed industrial solid residue after agar extraction by subcritical water treatment, *J. Appl. Phycol.* 33 (2021) 1181–1194, <https://doi.org/10.1007/s10811-020-02349-0>.
- [6] J. Zhang, C. Wen, H. Zhang, Y. Duan, H. Ma, Recent advances in the extraction of bioactive compounds with subcritical water: a review, *Trends Food Sci. Technol.* 95 (2020) 183–195, <https://doi.org/10.1016/j.tifs.2019.11.018>.
- [7] Ó. Benito-román, B. Blanco, M.T. Sanz, S. Beltrán, Subcritical water extraction of phenolic compounds from onion skin wastes (*Allium cepa* cv. Horcal): effect of temperature and solvent properties, *Antioxidants* 9 (2020) 1–18, <https://doi.org/10.3390/antiox9121233>.
- [8] P. Alonso-Riño, M.T. Sanz, Ó. Benito-Román, S. Beltrán, E. Trigueros, Subcritical water as hydrolytic medium to recover and fractionate the protein fraction and phenolic compounds from craft brewer's spent grain, *Food Chem.* 351 (2021), 129264, <https://doi.org/10.1016/j.foodchem.2021.129264>.
- [9] E. Trigueros, P. Alonso-Riño, C. Ramos, C.I.K. Diop, S. Beltrán, M.T. Sanz, Kinetic study of the semi-continuous extraction/hydrolysis of the protein and polysaccharide fraction of the industrial solid residue from red macroalgae by subcritical water, *J. Environ. Chem. Eng.* 9 (2021), 106768, <https://doi.org/10.1016/j.jece.2021.106768>.
- [10] G. Jiao, G. Yu, J. Zhang, H.S. Ewart, Chemical structures and bioactivities of sulfated polysaccharides from marine algae, *Mar. Drugs* 9 (2011) 196–223, <https://doi.org/10.3390/md9020196>.
- [11] A.S.A. Mohammed, M. Naveed, N. Jost, Polysaccharides: classification, chemical properties, and future perspective applications in fields of pharmacology and biological medicine (A review of current applications and upcoming potentialities), *J. Polym. Environ.* 29 (2021) 2359–2371, <https://doi.org/10.1007/s10924-021-02052-2>.
- [12] K. Samarakoon, Y.-J. Jeon, Bio-functionalities of proteins derived from marine algae - a review, *Food Res. Int.* 48 (2012) 948–960, <https://doi.org/10.1016/j.foodres.2012.03.013>.
- [13] A. Cassano, C. Conidi, R. Ruby-Figueroa, R. Castro-Muñoz, Nanofiltration and tight ultrafiltration membranes for the recovery of polyphenols from agro-food by-products, *Int. J. Mol. Sci.* 19 (2018) 351, <https://doi.org/10.3390/ijms19020351>.
- [14] S. Saidi, A. Deratani, M.-P. Belleville, R. ben Amar, Production and fractionation of tuna by-product protein hydrolysate by ultrafiltration and nanofiltration: impact on interesting peptides fractions and nutritional properties, *Food Res. Int.* 65 (2014) 453–461, <https://doi.org/10.1016/j.foodres.2014.04.026>.
- [15] X. Yu, L. Bogaert, R. Hu, O. Bals, N. Grimi, E. Vorobiev, A combined coagulation-ultrafiltration method for enhanced separation of proteins and polyphenols, *Separ. Sci. Technol.* 51 (2016) 1030–1041, <https://doi.org/10.1080/01496395.2016.1141957>.
- [16] M. Cissé, F. Vaillant, S. Bouquet, D. Pallet, F. Lutin, M. Reynes, M. Dornier, Athermal concentration by osmotic evaporation of roselle extract, apple and grape juices and impact on quality, *Innovat. Food Sci. Emerg. Technol.* 12 (2011) 352–360, <https://doi.org/10.1016/j.ifset.2011.02.009>.
- [17] C. Denis, A. Massé, J. Fleurence, P. Jaouen, Concentration and pre-purification with ultrafiltration of a R-phycoerythrin solution extracted from macro-algae *Grateloupia turuturu*: process definition and up-scaling, *Separ. Purif. Technol.* 69 (2009) 37–42, <https://doi.org/10.1016/j.seppur.2009.06.017>.
- [18] R. Mittal, A.G. Lamdande, R. Sharma, KSMS Raghavarao, Membrane processing for purification of R-Phycoerythrin from marine macro-alga, *Gelidium pusillum* and process integration, *Separ. Purif. Technol.* 252 (2020), 17470, <https://doi.org/10.1016/j.seppur.2020.117470>.
- [19] L. Zaouk, A. Massé, P. Bourseau, S. Taha, M. Rabiller-Baudry, S. Jubeau, B. Teychené, J. Pruvost, P. Jaouen, Filterability of exopolysaccharides solutions from the red microalga *Porphyridium cruentum* by tangential filtration on a polymeric membrane, *Environ. Technol.* 41 (2020) 1167–1184, <https://doi.org/10.1080/09593330.2018.1523234>.
- [20] A.K. Fard, G. McKay, A. Buekenhoudt, H. Al Sulaiti, F. Motmans, M. Khraisheh, M. Atieh, Inorganic membranes: preparation and application for water treatment and desalination, *Materials* 11 (2018) 1–47, <https://doi.org/10.3390/ma11010074>, 2018.
- [21] Y.S. Lin, Inorganic membranes for process intensification: challenges and perspective, *Ind. Eng. Chem. Res.* 58 (2019) 5787–5796, <https://doi.org/10.1021/acs.iecr.8b04539>.
- [22] A. Ambrosi, N.S.M. Cardozo, I.C. Tessaro, Membrane separation processes for the beer industry: a review and state of the art, *Food Bioprocess Technol.* 7 (2014) 921–936, <https://doi.org/10.1007/s11947-014-1275-0>.
- [23] M. Pinelo, G. Jonsson, A.S. Meyer, Membrane technology for purification of enzymatically produced oligosaccharides: molecular and operational features affecting performance, *Separ. Purif. Technol.* 70 (2009) 1–11, <https://doi.org/10.1016/j.seppur.2009.08.010>.
- [24] A.D. Marshall, P.A. Munro, G. Trägårdh, The effect of protein fouling in microfiltration and ultrafiltration on permeate flux, protein retention and selectivity: a literature review, *Desalination* 91 (1993) 65–108, [https://doi.org/10.1016/0011-9164\(93\)90047-Q](https://doi.org/10.1016/0011-9164(93)90047-Q).
- [25] H. Krawczyk, A. Arkell, A.-S. Jönsson, Membrane performance during ultrafiltration of a high-viscosity solution containing hemicelluloses from wheat bran, *Separ. Purif. Technol.* 83 (2011) 144–150, <https://doi.org/10.1016/j.seppur.2011.09.028>.
- [26] N.T.T. Doan, Q.D. Lai, Ultrafiltration for recovery of rice protein: fouling analysis and technical assessment, *Innov. Food Sci. Emerg. Technol.* 70 (2021), 102692, <https://doi.org/10.1016/j.ifset.2021.102692>.
- [27] L. Grossmann, S. Ebert, J. Hinrichs, J. Weiss, Production of protein-rich extracts from disrupted microalgae cells: impact of solvent treatment and lyophilisation, *Algal Res.* 36 (2018) 67–76, <https://doi.org/10.1016/j.algal.2018.09.011>.
- [28] E.A. Boss, R.M. Filho, E. C. Vasco De Toledo, Freeze drying process: real time model and optimization, *Chem. Eng. Process: Process Intensif.* 43 (2004) 1475–1485, <https://doi.org/10.1016/j.cep.2004.01.005>.
- [29] T. Moritz, S. Benfer, P. Arki, G. Tomandl, Influence of the surface charge on the permeate flux in the dead-end filtration with ceramic membranes, *Separ. Purif. Technol.* 25 (2001) 501–508, [https://doi.org/10.1016/S1383-5866\(01\)00080-6](https://doi.org/10.1016/S1383-5866(01)00080-6).
- [30] J. Hermia, Constant pressure blocking filtration laws - application to power-law non-Newtonian fluids, *Trans. Inst. Chem. Eng.* 60 (1982) 183–187, web: <http://hdl.handle.net/2078.1/57489>.
- [31] R.W. Field, D. Wu, J.A. Howell, B.B. Gupta, Critical flux concept for microfiltration fouling, *J. Membr. Sci.* 100 (1995) 259–272, [https://doi.org/10.1016/0376-7388\(94\)00265-Z](https://doi.org/10.1016/0376-7388(94)00265-Z).
- [32] M.C. Vincent-Vela, S. Álvarez, J. Lora, E. Bergantiños, Analysis of membrane pore blocking models adapted to crossflow ultrafiltration in the ultrafiltration of PEG, *Chem. Eng. J.* 149 (2009) 232–241, <https://doi.org/10.1016/j.cej.2008.10.027>.
- [33] T. Qi, X. Chen, W. Shi, T. Wang, M. Qiu, X. Da, J. Wen, Y. Fan, Fouling behavior of nanoporous ceramic membranes in the filtration of oligosaccharides at different temperature, *Separ. Purif. Technol.* 278 (2022), <https://doi.org/10.1016/j.seppur.2021.119589>, 119589.
- [34] J.B. Sluiter, R.O. Ruiz, C.J. Scarlata, A.D. Sluiter, D.W. Templeton, Compositional analysis of lignocellulosic feedstocks. 1. Review and description of methods, *J. Agric. Food Chem.* 58 (2010) 9043–9053, <https://doi.org/10.1021/jf1008023>.
- [35] V.L. Singleton, R. Orthofer, R.M. Lamuela-Raventós, Analysis of total phenols and other oxidation substrates and antioxidants by means of Folin-Ciocalteu reagent, *Methods Enzymol.* 299 (1999) 152–178, [https://doi.org/10.1016/S0076-6879\(99\)99017-1](https://doi.org/10.1016/S0076-6879(99)99017-1).
- [36] I.F.F. Benzie, J.J. Strain, The ferric reducing ability of plasma (FRAP) as a measure of "antioxidant power": the FRAP assay, *Anal. Biochem.* 239 (1996) 70–76, <https://doi.org/10.1006/abio.1996.0292>.
- [37] C. Jarusutthirak, G. Amy, J.P. Croué, Fouling characteristics of wastewater effluent organic matter (EfOM) isolates on NF and UF membranes, *Desalination* 145 (2002) 247–255, [https://doi.org/10.1016/S0011-9164\(02\)00419-8](https://doi.org/10.1016/S0011-9164(02)00419-8).
- [38] A.G. Fane, C.J.D. Fell, A review of fouling and fouling control in ultrafiltration, *Desalination* 62 (1987) 117–136, [https://doi.org/10.1016/0011-9164\(87\)87013-3](https://doi.org/10.1016/0011-9164(87)87013-3).
- [39] V. Lahoussine-Turcaud, M.R. Wiesner, J.-Y. Bottero, Fouling in tangential-flow ultrafiltration: the effect of colloid size and coagulation pretreatment, *J. Membr. Sci.* 52 (1990) 173–190, [https://doi.org/10.1016/S0376-7388\(00\)80484-6](https://doi.org/10.1016/S0376-7388(00)80484-6).
- [40] M.T. Alreshedi, O.D. Basu, Effects of feed water temperature on irreversible fouling of ceramic ultrafiltration membranes, *J. Water Proc. Eng.* 31 (2019), 100883, <https://doi.org/10.1016/j.jwpe.2019.100883>.
- [41] F.J. Benítez, J.L. Acero, A.I. Leal, Application of microfiltration and ultrafiltration processes to cork processing wastewaters and assessment of the membrane fouling, *Separ. Purif. Technol.* 50 (2006) 354–364, <https://doi.org/10.1016/j.seppur.2005.12.010>.
- [42] T. Cromey, S.-J. Lee, J.-H. Kim, Effect of elevated temperature on ceramic ultrafiltration of colloidal suspensions, *J. Environ. Eng.* 141 (2015), 04014096, [https://doi.org/10.1061/\(ASCE\)EE.1943-7870.0000931](https://doi.org/10.1061/(ASCE)EE.1943-7870.0000931).
- [43] Z. Sereš, J. Gyura, M. Eszterle, M. Djurić, Separation of non-sucrose compounds from syrup as a part of the sugar-beet production process by ultrafiltration with ceramic membranes, *Eur. Food Res. Technol.* 223 (2006) 829–835, <https://doi.org/10.1007/s00217-006-0276-2>.
- [44] T. Tsuru, S. Izumi, T. Yoshioka, M. Asaeda, Temperature effect on transport performance by inorganic nanofiltration membranes, *AIChE J.* 46 (2000) 565–574, <https://doi.org/10.1002/aic.690460315>.
- [45] R. Vegas, A. Moure, H. Domínguez, J.C. Parajó, J. R. Álvarez, S. Luque, Purification of oligosaccharides from rice husk autohydrolysis liquors by ultra- and nano-filtration, *Desalination* 199 (2006) 541–543, <https://doi.org/10.1016/j.desal.2006.03.124>.
- [46] A. Giacobbo, M. Oliveira, E.C.N.F. Duarte, H.M.C. Mira, A.M. Bernardes, M.N. de Pinho, Ultrafiltration based process for the recovery of polysaccharides and polyphenols from winery effluents, *Separ. Sci. Technol.* 48 (2013) 438–444, <https://doi.org/10.1080/01496395.2012.725793>.
- [47] H. Tsihranska, G.A. Peev, B. Tylkowski, Fractionation of biologically active compounds extracted from propolis by nanofiltration, *J. Membr. Sci. Technol.* 1 (2011) 1–5, <https://doi.org/10.4172/2155-9589.1000109>.
- [48] G.D. Arend, W.T. Adorno, K. Rezzadori, M. Di Luccio, V.C. Chaves, F.H. Reginatto, J.C.C. Petrus, Concentration of phenolic compounds from strawberry (*Fragaria X*

- ananassa Duch) juice by nanofiltration membrane, *J. Food Eng.* 201 (2017) 36–41, <https://doi.org/10.1016/j.jfoodeng.2017.01.014>.
- [49] B. Díaz-Reinoso, A. Moure, H. Domínguez, J.C. Parajó, Ultra- and nanofiltration of aqueous extracts from distilled fermented grape pomace, *J. Food Eng.* 91 (2009) 587–593, <https://doi.org/10.1016/j.jfoodeng.2008.10.007>.
- [50] M. Plaza, M. Amigo-Benavent, M.D. del Castillo, E. Ibáñez, M. Herrero, Neof ormation of antioxidants in glycation model systems treated under subcritical water extraction conditions, *Food Res. Int.* 43 (2010) 1123–1129, <https://doi.org/10.1016/j.foodres.2010.02.005>.
- [51] F. Gu, J.M. Kim, K. Hayat, S. Xia, B. Feng, X. Zhang, Characteristics and antioxidant activity of ultrafiltrated Maillard reaction products from a casein-glucose model system, *Food Chem.* 117 (2009) 48–54, <https://doi.org/10.1016/j.foodchem.2009.03.074>.